

In-situ Synchrotron X-ray Microdiffraction Study of Lattice Rotation in Polycrystalline Materials during Uniaxial Deformations

H.D. Joo^{*}, K.H. Kim[†], C.W. Bark^{*}, Y.M. Koo^{*}, N. Tamura[‡]

^{*} *Materials Sci. & Eng., Pohang University of Science and Technology, Pohang 790-784, South Korea,*

[†] *Samsung Advanced Institute of Technology, P.O. Box 111, Suwon 440-600, South Korea*

[‡] *Lawrence Berkeley National Laboratory, University of California, 1 Cyclotron Road, Berkeley, CA 94720, USA*

ABSTRACT

Recent experiments have shown that formation of dislocation cell structures and rotation of structural elements at the macroscopic level are fundamental to the development of plastic deformation. However, attention should also be focused on micro-volumes because local stress and strain can significantly differ from their averaged values at the macroscale. *In-situ* orientation measurements in copper polycrystals during uniaxial deformation were performed using synchrotron x-ray microdiffraction at the Advanced Light Source. We observed heterogeneities in deformation-induced microstructure within individual grains. Different slip systems in particular can be simultaneously activated among neighboring volume elements of individual grains.

§1. INTRODUCTION

In order to understand the texture development during plastic deformation, experiments have recently focused on measuring deformation of polycrystalline materials at both the macroscopic and microscopic level. It has been reported that the plastic deformation of solids leads to the formation of dislocation cell structures as well as to the rotation of structural elements.[1,2] At the microscopic level, plastic deformation occurs almost exclusively through the motion of dislocations, resulting in the rotation of crystallographic lattice of grains. Therefore, attention should focus on deformed material microvolumes. Because the local stress and strain differ from those averaged values at macroscale, deformation heterogeneities should account for the rotation of different micr-fragments which contains subgrains, grains, etc., which play an important role in plasticity. Moreover, to our knowledge, *in-situ* studies of deformation behavior in polycrystalline material during deformation at the microscopic level have never been performed. In the present work, we investigate lattice rotation behavior in copper polycrystals during an in-situ deformation experiment at the microscopic level using x-ray microdiffraction.

Notation: Slip planes and directions are referenced according to the Schmid and Boas notation.[4]

Plane \Rightarrow B={111}, A= $\bar{1}$ 11, C= $\bar{1}$ $\bar{1}$ 1, D={1 $\bar{1}$ 1}; direction \Rightarrow I=[011], II=[0 $\bar{1}$ 1], III=[101], IV= $\bar{1}$ 01, V=[1 $\bar{1}$ 0], VI=[110]

§2. EXPERIMENTAL PROCEDURE

The material used in the present study was a 99.999% polycrystalline copper. A tensile sample, with a 7.5 mm gauge length and a 2 mm x 0.5 mm cross-section, was prepared by spark-erosion cutting. After mechanical polishing, the sample was annealed and chemically polished. We used synchrotron X-ray microdiffraction end-station on beamline 7.3.3 at the Advanced Light Source (ALS) to perform *in-situ* micro-diffraction experiments [3]. Due to the 45° incidence of the X-ray, the actual beam size at the sample position was 1.5 μm * 1.5 μm . In order to map the orientation and strain/stress distributions for each strain (0, 2, 4, 6, 8, 10, 15, 20, 25% strain), the same area on the sample was repeatedly raster scanned with the x-ray microbeam with a step size of 4 microns. The samples were elongated by a tensile device mounted on the translation stage with a strain rate of $2.22 \times 10^{-4} \text{ s}^{-1}$.

§3. RESULTS AND DISCUSSIONS

Diffraction patterns obtained from sample different positions were indexed and the orientation matrices were deduced. The orientation distributions of the area of interest in the copper samples at 0 and 6% strain are shown in Fig. 1(a)~(c). The orientation scale range has been modified to capture the orientation variations within the central grain at Fig.1(b)~(c). The misorientation measured within the central grain before loading is less than 0.1 degree, and increases in function of the applied tensile strain. We observed a higher variation in orientation by increasing strain in the middle of the center grain than at other positions within this grain. In order to fully capture the intragranular heterogeneities of deformation-induced microstructure, we monitored the tensile axis direction at 5 different points labeled A,B,C,D and E within the central grain (Fig. 1(a)). We also consider the relative motion of the tensile axes from their initial orientations as plastic deformation occurs. The rotation angle from initial position as a function of strain was plotted in Fig. 1(d). The tensile axis rotation at position A is much higher than that at position D. This position dependence is caused by the effect of the nearest neighbor grains. The angles between the central grain and G1, G2, G3, G4, G5, G6, G7, and G8 grains are 9.8, 3.3, 37, 21, 24, 36, 17, and 6.0 degrees, respectively. The initial orientations of grains G2 and G8 close to the A position of the central grain are similar to that of the central grain, while the angle between grains G5, G6 and the central grain, respectively, close to the D and B positions, are quite

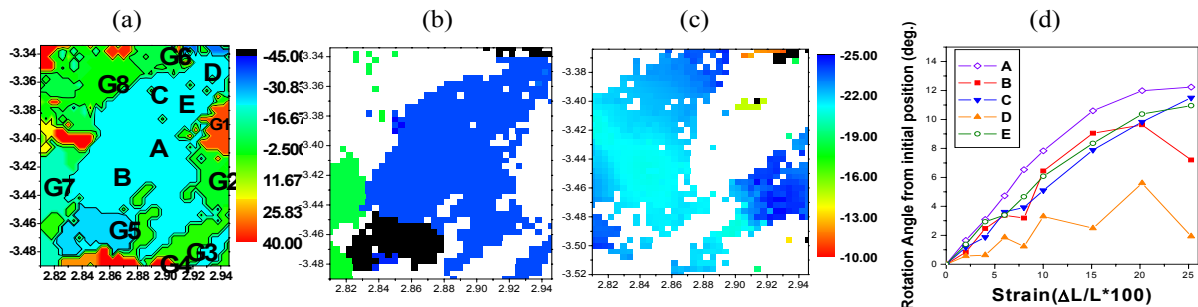


Figure 1. (a) shows the orientation map of the area of interest in the polycrystalline Cu sample and positions of 5 points, where the y direction is the sample tensile direction, (b) and (c) shows the change of orientation distribution of the central grain at 0 and 6% strain, respectively. (d) Rotation angle from initial position as a function of strain at each strain.

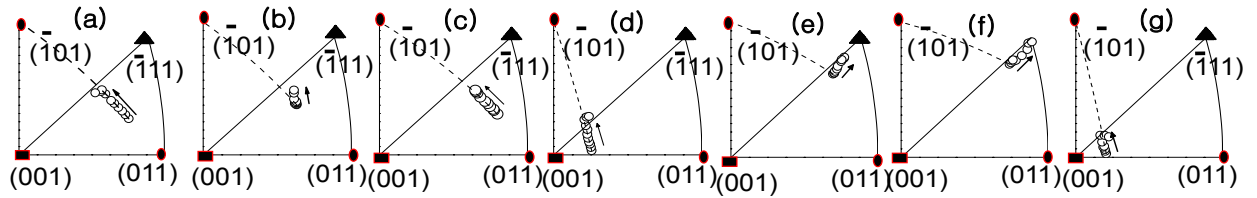


Figure 2. Tensile axis movement of the center grain in the 001 stereographic projection (a) A and those of neighboring grains (b) G1, (c) G2, (d) G3, (e) G4, (f) G5, and, (g) G6, where the open circles are experimental data and the dotted line is the tensile axis path expected by Schmid's law [4].

large. The grain boundaries in the diagonal direction linking G2, the central grain and G8 are therefore small angle boundaries. This phenomenon can be explained by the simultaneous selection of different acting slip systems in different parts within the grain. Lattice rotation near high angle grain boundary is small while lattice rotation near the low angle grain boundary is large, which means that grain boundaries and grain orientations affect slip behavior. The motion of the tensile axis at A points in the center grain is described in the 001 stereographic projection in Fig. 2(a), where open circles show the experimental data, while the dotted line represents the expected path for the tensile axis as predicted by Schmid's law[4]. Tensile axis movements like that of position A, follow expected classical theory tensile axis paths, but rotation angles varied differently. According to Schmid's law, initially activated slip systems in single crystals would have the highest Schmid factor [4]. The tensile axis follows the expected path for the BIV(111)[$\bar{1}01$] slip system (described by the Schmid and Boas notation.[4]), as in a single crystal but the total rotation angle from the initial orientation depends on the location within the grain. Our observations show that in many cases there is a clear deviation from the Sachs model prediction of the motion of the tensile axis. The Sachs model also fails to predict the activation of multiple slip systems within grains. The rotations of the tensile axis were also measured in other grains surrounding the central grain. Stereographic projections of neighbor grains are shown in Fig 2(b)~(g) where the initial orientation and their strain-induced rotations were determined for each grain. The tensile axis motions of all grains except G4 and G5 follow the line connecting the tensile axis to the primary slip direction [$\bar{1}01$]. As can be seen in Fig 2(e),(f), the behavior of grains G4 and G5 do not follow the theory, but show the unexpected activation of the BV(111)[$\bar{1}\bar{1}0$] slip system.

The streaking of diffraction patterns is considered in order to investigate the type of geometrically necessary

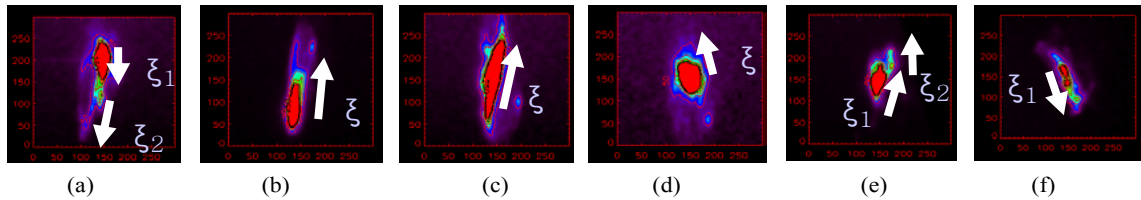


Figure 3. Laue images of the (111) reflection in the CCD plane for 8% strained Cu crystals. (a), (b), (c), (d), (e), and (f) are the reflection of the A, B, D, and E position of the central grain, G4 and G5 grain, respectively. The calculated Burgers vector (b) and dislocation line vector (τ) are (a) $b_1//[011]$, $\tau_1//[2-11]$, $b_2//[-110]$, $\tau_2//[11-2]$, (b) $b_1//[011]$, $\tau_1//[2-11]$, (c) $b_1//[101]$, $\tau_1//[1-2-1]$, (d) $b_1//[-101]$, $\tau_1//[1-21]$, (e) $b_1//[101]$, $\tau_1//[12-1]$, $b_2//[-101]$, $\tau_2//[11-2]$, (f) $b_1//[-101]$, $\tau_1//[1-21]$.

unpaired dislocation. The dislocation structure was analyzed based on the approach described by Barabash *et al.*[6]. In fcc crystals, there are 12 slip systems which have typical edge dislocation lines parallel to the direction of $\langle 112 \rangle$ with Burgers vector parallel to the glide direction $\langle 110 \rangle$ and with corresponding glide planes $\{111\}$. Several Laue peaks with streaking axes parallel to $\xi = \tau \times \mathbf{g} / |\tau \times \mathbf{g}|$, where τ is the dislocation line vector and \mathbf{g} is the momentum transfer vector. The streaking directions are simulated about the 12 most likely edge dislocation systems and compared with the experimental one. In this way, we determined the kind of dislocation system, as shown in Fig.3. Unpaired dislocations piled-up in the A position of the central grain has a Burgers vector $\mathbf{b}=[011]$, dislocation line $\tau=[2\bar{1}1]$ and slip plane $n=(\bar{1}\bar{1}1)$ which corresponds to the CI slip system. Reflection tail Dislocation systems correspond to BIV and CIII, that is, multi-slip systems which have been activated. Tensile axis rotations of 5 other positions also follow the BIV slip system, but there is little deviation which results from multi-slip. The dislocations system of B, D, and E position in the central grain correspond to CI, CIII, and BIV slip systems, respectively. The FWHM of reflections in B and D positions is larger than that in A and E, which means that the density of geometrically necessary dislocation A and E is much lower. Angles between center grain and G5 (G6), close to B(D) position, are 24.3(35.6) degrees, and dislocation glide through the grain boundary is more difficult than through other grains. Therefore, many dislocations pile up near G5 and G6 grains than other grains. The dislocation in grain 4 corresponds to the BV and AIII slip systems, and this is coincident with tensile axis rotation data.

In summary, we have investigated the effect of neighboring grains on intra-/inter-granular plastic deformations during uniaxial deformation by *in-situ* observation of local lattice rotation and diffraction peak streaking.

ACKNOWLEDGEMENTS

This work was supported by the Research Institute of Industrial Science & Technology and the National Program for Tera-level Nanodevices of the Ministry of Science & Technology as one for the 21st century Frontier Program and the authors wish to express appreciation for financial support. We thank R.S. Celestre and W.A. Caldwell for their assistance in performing the Microdiffraction experiment at the Advanced Light Source. The Advanced Light Source is supported by the Director, Office of Science, Office of Basic Energy Sciences, Materials Sciences Division, of the U.S. Department of Energy under Contract No. DE-AC03-76SF00098 at Lawrence Berkeley National Laboratory.

Reference

1. Hansen, N., *Mater. Sci. Engng*, **6**, pp. 1039, (1990)
2. Gernov S. A., Hamana D., Dvorovienko N. A., Golayev V. I., and Tehmutov V. M., *Phil. Mag. Lett*, **78**, pp. 185 (1998)
3. MacDowell A. A., Celestre R. S., Tamura N., Spolenak R., Valek B., Brown W. L., Bravman J. C., Padmore H. A., Batterman B. W. and Patel J. R., *Nuclear inst. Meth.*, **467-468**, pp. 936 (2001)
4. Schmid, E., and Boas, W., *Plasticity of Crystals* (London: Chapman & Hall); translation of original 1935 German edition, 1968
5. E. Schmid and N. Boas, *Kristall. Plastizitat*, Berlin (1961)
6. R.I. Barabash, G.E. Ice, and F.J. Walker, *J. Appl. Phys.*, **93**, pp. 1457-1464, (2003)